Geologia Croatica
Journal of the Croatian Geological Survey and the Croatian Geological Society

2024 | 77/3 | 235–242 | 5 Figs. | 1 Supplement |

www.geologia-croatica.hr

Deciphering rock surface origins in a karst cave: insights from the Rača Cave, Lastovo, Croatia

Georgios Lazaridis[1,*], Konstantinos P. Trimmis[2], Ivan Drnić[3] and Kristina Brkić Drnić[4]

[1] Aristotle University of Thessaloniki, Faculty of Sciences, School of Geology, 54124 Thessaloniki, Greece; (*corresponding author: geolaz@geo.auth.gr)
[2] University of Bristol, Department of Anthropology and Archaeology, 43 Woodland Road, BS8 100 Bristol, UK
[3] Archaeological Museum, Trg Nikole Zrinskog 19/1, 10000 Zagreb, Croatia
[4] University of Zadar, Department of Archaeology, Ulica Mihovila Pavlinovića 1, 23000 Zadar, Croatia

doi: 10.4154/gc.2024.13

Article history:
Manuscript received: August 22, 2023
Revised manuscript accepted: June 04, 2024
Available online: October 02, 2024

Keywords: cave survey, 3D scanning, structural analysis, Adriatic Sea, Dinarides, speleogenesis, dissolution, breakdown

Abstract

This paper outlines a comprehensive fieldwork methodology for discerning the origin of rock surfaces within a karst cave environment. This methodology is particularly utilized in a cave with breakdown morphology. Using Rača Cave in Lastovo, Croatia as a case study, we explore geological and morphological features through advanced surface analysis. The approach involves meticulous measurement of rock discontinuities, joint patterns, and surface formations. Cost-efficient and time-efficient data collection and processing during field-work were undertaken with FieldClino Move and Polycam applications on smartphones. Visualization techniques were employed to elucidate the interplay between erosion, deposition, and speleogenetic processes.

1. INTRODUCTION

Karst caves are formed in carbonate rocks mainly due to a process of rock removal by dissolution when water circulates underground and interacts with the carbonates (e.g. FORD & WILLIAMS, 2007). This process leaves behind empty spaces with shapes and morphological features that are informative of the various parametres that guide the process of speleogenesis, namely the hydrology, chemistry and availability of rock fractures and discontinuities. Other agents can additionally contribute to the formation of caves including erosion in mainly well-formed mature cave systems (e.g. FARANT & SMART, 2011), breakdown when physical conditions are favourable for ceiling collapse (e.g. WHITE & WHITE, 2000; OSBORNE, 2002), or condensation corrosion by water that condenses on the rock surface when it is colder than the air (e.g. DREYBRODT et al., 2005; GABROVŠEK et al., 2010). A process-based classification of caves can be found in LAZARIDIS (2022). All these various processes are amalgamated during speleogenesis and they shape the expansion of the cave space. They can act simultaneously or in successive phases of development with variations in their intensity.

The resulting morphology of each agent is predictable and can be investigated in the karst cave environment. This is the key to identifying morphological features at various scales when understanding speleogenesis. Large-scale features including the ground plan pattern are related to the speleogenetic phases, whereas features in the dimensions of passages or even smaller openings are relatively susceptible to phase changes and mainly reflect events of various cave modifications such as corrosion by invasive water, erosion, condensation corrosion, and collapse (e.g. LAURITZEN & LUNDBERG, 2000).

However, when it comes to studying these forms various factors obscure observations and interpretations. These are mainly depositional phases of clastic and chemical sediments that cover the floor and the upper part of the cave passages, respectively.

To summarise, the following surfaces can be observed in caves and studied to understand their development:

- Dissolution surfaces of the carbonate rock due to flowing underground water
- Dissolution surfaces due to condensation corrosion that re-sculpt wall-rocks and speleothems
- Surfaces that correspond to bedding planes and rock fractures revealed after breakdown events
- Depositional features
- Erosional *sensu lato* surfaces that correspond to paragenesis (e.g. PASINI, 2009).

The complexity of these processes and their interaction can make the identification and discrimination of the various morphological features during fieldwork challenging and sometimes questionable.

This was the case during fieldwork in the archaeological Rača Cave in Croatia. The first impression when entering the cave is that it is formed due to collapse favoured by the intermediate dip-angle of the bedding planes. The goal of this research is to identify speleogenetic processes and to distinguish the cause-and-effect relationship of primary structural elements (bedding, faults) with the occurrence of different dissolution and depositional forms in the speleological object. To investigate, identify, and visualize specific surfaces we combined measurements of the orientation of a large number of structural elements, dissolution features, together with 3D scanning of the cave.

2. GEOLOGICAL SETTING

Lastovo Island is located in the vicinity of a notable seismically active area (e.g. GARAŠIĆ, 2021). Along with 45 other smaller islands, it forms the Lastovo Archipelago, where Upper Jurassic to mid-Cretaceous limestones were deposited on the Adriatic carbonate platform (VLAHOVIĆ et al., 2002). The karst landform of the area was formed after the Alpine orogeny (VLAHOVIĆ et al., 2005; KORBAR, 2009) that shaped the area, due to the exogenous processes. Most of the continental karst caves in Croatia are of vertical development (GARAŠIĆ, 1991), whereas most of the submerged caves are horizontally developed (SURIĆ et al., 2010). Late Jurassic mudstone and wackestone are the oldest rocks that crop out on the island. A fault running along the northern shoreline of the island distinguishes the younger carbonate rocks from the older succession (SOKAČ et al., 2014). The island's landscape features the presence of karst depressions and formations such as poljes and karren.

3. CAVE DESCRIPTION

Rača cave is located on the island of Lastovo at 140 m asl (N42˚ 44´ 05´´, E016˚ 54´ 38´´ WGS84; Fig. 1a), and is the largest recorded cave on the island to date (MARJANAC, 1956; DRNIĆ & BRKIĆ DRNIĆ, 2023). The cave's developmental orientation aligns along a W-E axis, and its entrance is a result of breakdown processes (refer to Fig. 1b). The initial chamber stands as the largest, while subsequent chambers are demarcated by the presence of speleothem depositions, which take shape as expansive columns and flowstone. Small windows formed amidst the speleothems establish interconnections between different areas of the chambers. Notably, the vertical span of the cave measures ~17 metres. Enclosing the cave's ground plan, the minimum encompassing rectangle spans dimensions of ~73 metres by ~20 metres, as extracted from the 3D scan.

Within the cave, the floor is covered with clastic sediments, forming a cone of debris near the entrance. As one ventures towards the cave's depths, the sediment-laden floor assumes a relatively horizontal disposition. Subsequent chambers exhibit progressively lower elevations above sea level. The ceiling primarily consists of flat inclined surfaces. Dominating the central expanse of the cave, substantial speleothems such as stalagmites and columns partition the various chambers. These formations exhibit signs of breakage, characterized by an array of cracks, some of which are filled with calcite deposits.

In the entrance zone, it can be observed and should be noted, that these formations display evidence of corrosion attributed to condensation processes. However, in the cave's more profound recesses, the speleothems appear unaffected by this corrosive phenomenon, either covered by calcite encrustations stemming from stagnant water or otherwise not subjected to this specific process.

4. METHODOLOGY

To identify and visualize dissolution surfaces within the cave, the approach involved creating a comprehensive dataset of rock discontinuities in the limestone above the cave. This dataset encompasses measurements of dip direction and dip angle for both bedding planes and rock fractures, such as joints. These measurements were meticulously acquired using the FieldMove Clino application by Midland Valley (Petroleum Engineering and Structural Geology Software), after checking the calibration of the smartphone’s sensors (magnetometer/gyroscope/accelerometer; see software’s manual at www.petex.com). The collected data were associated with the "limestone" unit utilized in our analysis. Subsequently, random measurements were conducted within the cave, correlating with a designated unit termed "cave". Notably, these measurements were taken on exposed surfaces devoid of speleothem coverings and were distributed throughout the cave's extent.

The next phase involved projecting and comparing the two datasets on a unified stereo net diagram and scatter diagram. The scatter diagram served to establish the 99% confidence interval ellipses for bedding planes and the pair of joint sets defined within the limestone unit. Plot and confidence intervals are drawn in PAST software (HAMMER et al., 2001). For classification purposes, any measurements from the "cave"

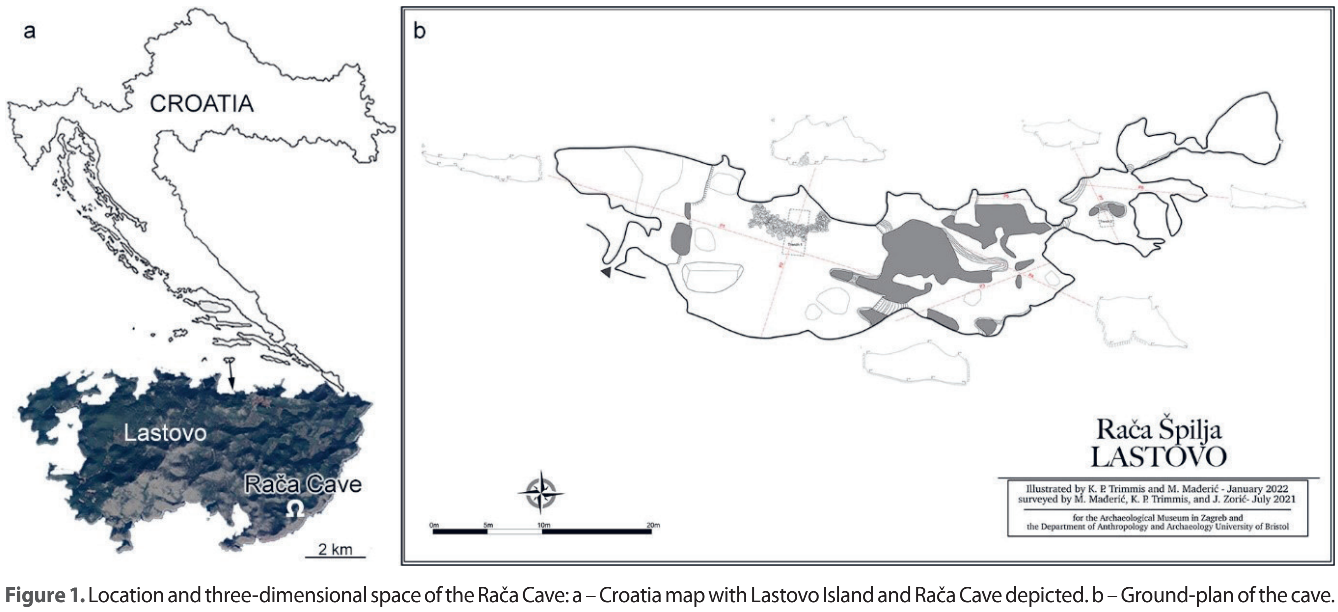

Figure 1. Location and three-dimensional space of the Rača Cave: a – Croatia map with Lastovo Island and Rača Cave depicted. b – Ground-plan of the cave.

dataset that overlapped with the range of the "limestone" dataset were categorized as breakdown surfaces. Conversely, measurements outside this range were indicative of dissolution processes. To comprehensively document these features, we utilized photo documentation and 3D modelling techniques employing the 3D scanner application and LiDAR sensors integrated into the iPhone 14 Pro. With respect to the mapping grades of the International Union of Speleology (UIS) as given in HÄUSELMANN (2011), the survey has the possibility to provide scans that are reliable to a single centimetre (ZACZEK-PEPLINSKA & KOWALSKA, 2022) and although variable, they easily fit grade 5 and, in many cases, can reach the prerequisites for grade 6. Map detail grade corresponds to 4, which is the maximum detail, and regarding qualifications the suffixes B to F fit to this method (HÄUSELMANN, 2011).

In terms of qualitative assessment, various criteria were employed to distinguish different sections of side walls and ceilings see Supplement:

- Condensation corrosion was discerned through observed cuts in speleothems, which formed cupolas or similar pockets
- Breakdown surfaces were typified by a flat ceiling following bedding planes, angular connections between planar surfaces, and abrupt terminations of adjacent smooth dissolution pockets
- Surfaces not aligning with the aforementioned criteria commonly pertained to dissolution stages of speleogenesis and could exhibit attributes including cupolas, scallops, flutes, pendants, and more
- Furthermore, surfaces linked to erosion *sensu lato*, referred to as paragenesis, were discerned by their distinctive dissolution forms. These features were intricately connected with specific cave passages and micro-scale morphologies. Notable examples encompassed paragenetic pendants, meandering paragenetic canyons, lateral notches with half-tube configurations, and scallops (FARRANT & SMART, 2011; LAURITZEN & LAURITSEN, 1995).

5. RESULTS AND DISCUSSION

Caves represent underground voids that emerge through distinct geological and biological processes (refer to LAZARIDIS, 2022, for a formal definition). These spaces are delineated by boundaries (CURL, 1964), referred to as surfaces throughout the text, and are intimately linked to the direct action of speleogenetic processes. Examining these surfaces facilitates the identification of various events and agents responsible for their creation, encompassing both erosional and depositional manifestations. Although this methodology primarily concentrates on surfaces with erosional characteristics, it's important to recognize that both types of surfaces offer crucial insights into comprehending cave evolution.

We meticulously measured rock discontinuities (n=52) of thick-bedded limestone on the surface above the cave and at a distance of about 50 metres from the cave entrance (Fig. 2). In this area, where the limestone crops out, we recognized bedding planes, exhibiting an average dip direction and angle of 12°/14° and two groups of joints: J1: 184°/50° and J2: 111°/72°.

Within the cave's interior, we conducted measurements on arbitrary rock surfaces (n=139), deliberately avoiding those concealed by speleothems. These measurements were plotted on the stereonet diagram illustrated in Fig. 3a. While an overlap between the two datasets is evident, it is noteworthy that a substantial number of cave surfaces do not align with the orientations of rock discontinuities.

In pursuit of deeper insight, we further projected all data onto the scatter diagram shown in Figure 3c. correlating strike with dip angle. As anticipated, the two datasets display partial overlap. Ellipses on this diagram represent the 99% confidence interval (the percentage of the population that falls in these ellipses), underscoring that surfaces falling within these ellipses cannot be rejected as belonging to the rock's discontinuities, at a level of significance α=0.01. The shared domain between the "cave" dataset and the "limestone" dataset signifies surfaces that reasonably align with bedding planes

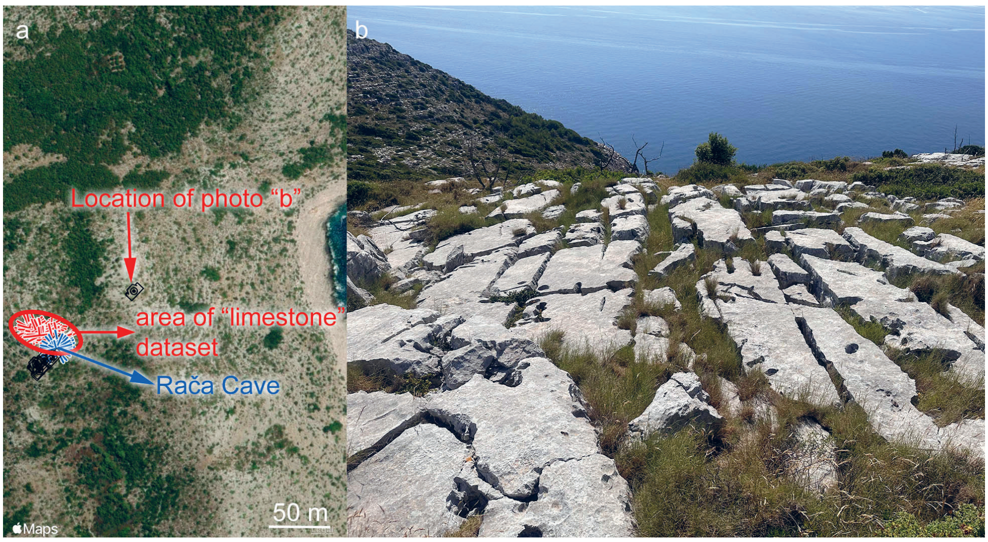

Figure 2. a. location of the entrance of Rača Cave and the area where "limestone" dataset of rock discontinuities was measured. b. characteristic appearance of the limestone in the cave surroundings.

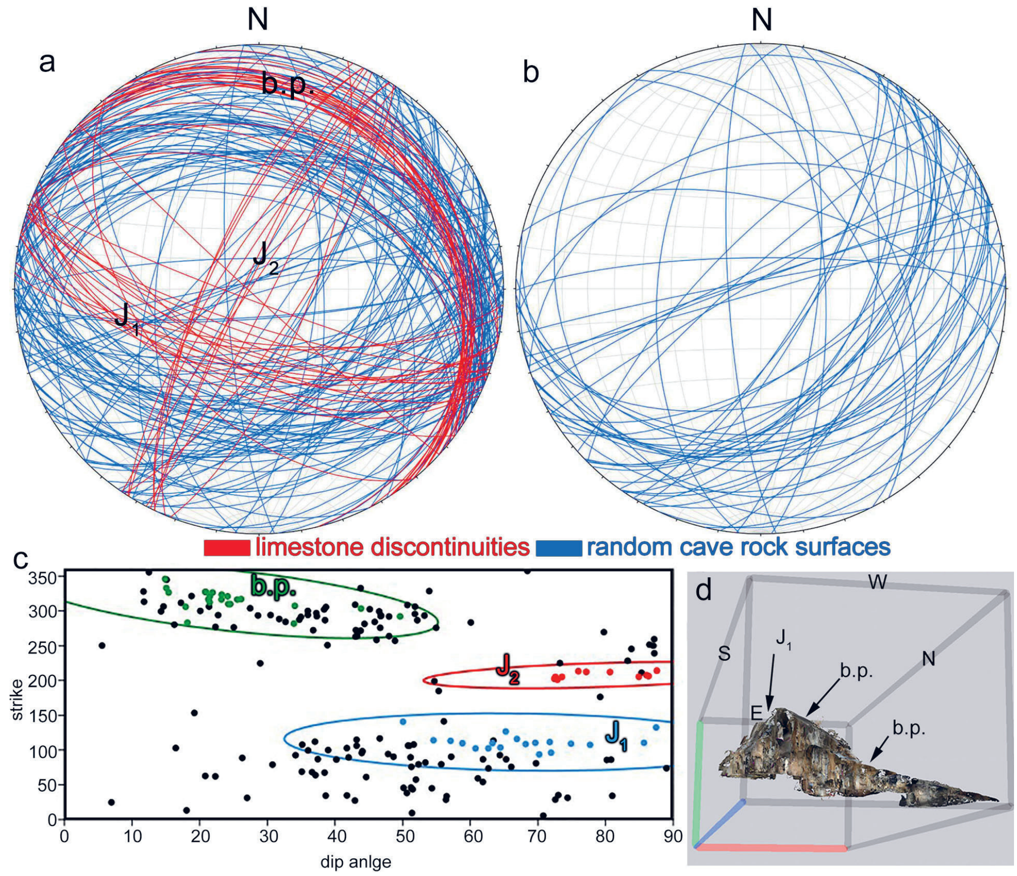

Figure 3. Analysis of "limestone" and "cave" datasets from Rača Cave. a – Rock discontinuities and random rock surfaces of the cave boundaries are plotted together: bedding planes (b.p.), and two joint sets J_1 and J_2 are indicated. b – random rock surfaces that correspond to dissolution surfaces; data for which the hypothesis to belong to limestone discontinuities cannot be rejected have been excluded (see Fig. 5 and text). c – Scatter diagram of the "limestone" and "cave" datasets analysed from Rača Cave. Coloured dots and ellipses of 99% confidence intervals are plotted for the "limestone" dataset that consists of the group of bedding planes (b.p.; green dots) and joint sets J_1 (blue dots) and J_2 (red dots). Black dots represent the "cave" dataset of random rock surfaces that define the cave boundaries. d – SW view of the cave, where the ceiling defined by bedding planes (b.p.) and the walls defined by joints (J_1) can be observed (see text).

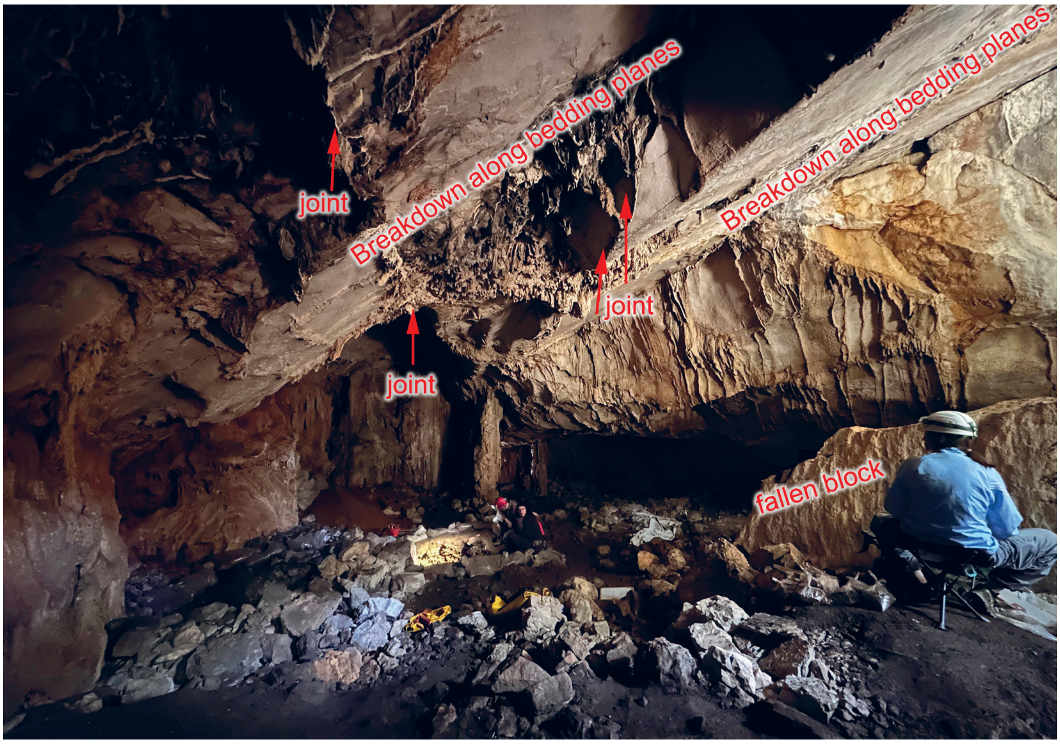

Figure 4. The first and largest chamber of Rača Cave, with ceiling surfaces dominated by breakdown surfaces along bedding planes and joints of the limestone.

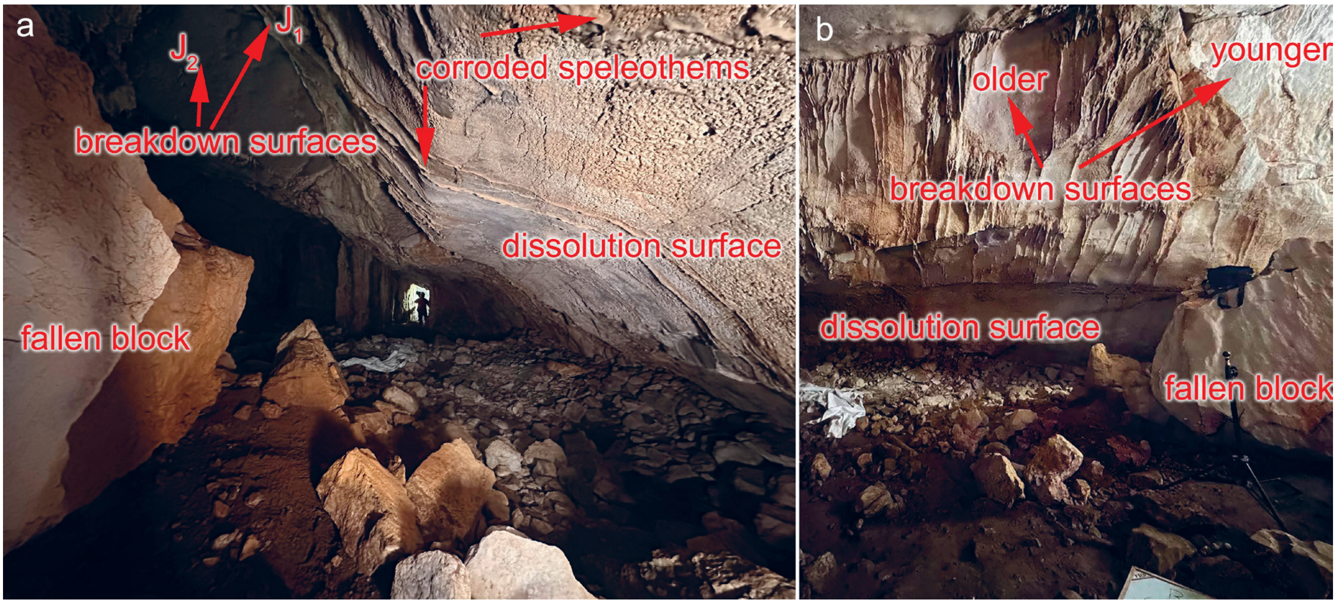

Figure 5. a – Illustration of a dissolution surface at the lower part of the first chamber in Rača Cave and how it is associated with breakdown surfaces and corroded speleothems by condensation corrosion. b – The same spot observed from the northern part of the first chamber, where breakdown surfaces of two different events can be observed.

and joints originating from breakdown events. Qualitatively, these surfaces significantly contribute to the definition of the cave's contours, a characteristic demonstrated in the three-dimensional cave model showcased in Figure 3d. and in Figure 4. of the first chamber.

Considering both the quantitative findings and qualitative observations, the overall morphology of Rača Cave distinctly exhibits characteristics associated with collapse formations (Fig. 4).

Within diverse insular environments, such as Mallorca, a range of cave classifications are discernible, encompassing "vadose shafts," "vadose located caves," "phreatic caves," and "insular caves" (as described by GINÉS, 1995). Notably, breakdown caves are prevalent within the category of "vadose located caves." These cases comprise segments, where the original cave boundaries undergo transformation due to the dislodgment of blocks from the ceiling or walls. This phenomenon, coupled with the deposition of speleothems, often muddles observations and complicates speleogenetic interpretations. It is worth noting that numerous other cave types, such as structurally controlled caves, conduit-caves, network caves, and mechanical shafts, as discussed by GINÉS (1995), commonly exhibit sections influenced by breakdown-related alterations.

Rača Cave, while predominantly showcasing breakdown characteristics, appears to offer indications of processes beyond mere breakdown. As delineated in Figure 3c., several surfaces deviate from the 99% confidence interval designated for limestone discontinuities. This subset of the dataset is projected on the stereonet of Figure 3b. and is indicative of dissolution surfaces, with the caveat that paragenetic features lack qualitative verification. These surfaces predominantly define the southern segments of the cave and manifest as relatively diminutive cupolas adorning the cave ceilings or resemble a long smooth and curved surface that extends along the long axis of the cave (Fig. 5). Speleothems formed within these regions exhibit signs of condensation corrosion (Fig. 5a), signifying some degree of modification resulting from this process. Such surfaces are delimited upwards to breakdown surfaces. Old and younger breakdown events can be recognized by differences in the smoothness of the surfaces (Fig. 5b), indicating that this process took place in multiple events.

Various methodologies that relate structural analysis, cave morphology, cave morphometry and hydrogeology have been introduced and applied on numerous caves and karst systems (e.g. PLAN et al., 2009; PICINI, 2011; JOUVES et al., 2017; SZCZYGIEŁ et al., 2022; DORA et al., 2023) in order to investigate their speleogenesis. However, in the case of Rača Cave, these methods had limitations or cannot even be applied due to the extent of breakdown morphology. That means in every explored passage of the cave the dominant features are related to collapse. The origin of the very few dissolution features that were identified is speculative. The general shape of the cave exhibits an E-W elongation, affected by the joint sets J1 and the bedding planes. According to studies on cave development and active tectonics, (so-called cavitonics), cave passages tend to be developed perpendicular to the extensional component of the stress field (LITTVA et al., 2015; SHANOV & KOSTOV, 2015; LAZARIDIS et al., 2024) and this conforms to the orientation of the nontectonic E-W structures in the broader area (MARINČIĆ, 1997).

Regarding the employed fieldwork techniques, it's important to highlight that the capability to gather and promptly visualize data significantly and instantly enhanced our comprehension of the diverse morphological surfaces within the cave. Furthermore, the concurrent generation of 3D models (Fig. 1b) facilitated the documentation of these characteristics, emerging as a comprehensive tool for cave site investigation. By enabling observations from multiple perspectives and presenting the cave as a cohesive entity, this approach transcended the practice of examining individual segments in isolation.

6. CONCLUSIONS

It's not uncommon for breakdown morphology to obscure the clear identification of features associated with the dissolution stages of speleogenesis. Through our analysis, we have presented compelling evidence for the existence of additional processes within Rača Cave, a site predominantly characterized by breakdown formations. The manifestation of these processes becomes evident through the presence of dissolution surfaces, which exhibit a statistically significant distinction from the rock discontinuities. These distinctions are effectively visualized using scatter diagrams. By employing qualitative criteria, we have successfully identified condensation corrosion and particular original phreatic features. The selected tools not only proved to be time-efficient but also enabled engagement in real-time data visualization while perceiving the cave's morphology as a cohesive entity.

In its entirety, our fieldwork analysis has provided a comprehensive understanding of various intricacies related to the surfaces that delineate the boundaries of the cave. Moreover, this analysis has enabled us to perform statistical comparisons of datasets, thereby attributing a level of significance to our observations.

ACKNOWLEDGMENT

We sincerely thank the Anonymous Reviewers for their constructive comments, which greatly contributed to the improvement of our paper.

REFERENCES

CURL, R.L. (1964): On the definition of a cave.– Bulletin of National Speleological Society, 26, 1, 1−6.

DORA, D., LAZARIDIS, G., VOUVALIDIS, K., TOKMAKIDIS, K. & VENI, G. (2023): Morphometric Analyses of Greek Caves: How Morphology Predicts Cave Origin.– Bulletin of the Geological Society of Greece, 60/1, 14–26. doi: 10.12681/bgsg.34887

DREYBRODT, W., GABROVŠEK, F. & PERNE, M. (2005): Condensation Corrosion: A Theoretical Approach.– Acta Carsol., 34/2, 317–347. doi: 10.3986/ac.v34i2.262

DRNIĆ, K.B. & DRNIĆ, I. (2023): An island in the heart of the Adriatic Sea – finds from the Rača cave on the island of Lastovo.– In: DRNIĆ, K.B., TRIMMIS, P.K. & DRNIĆ, I. (eds): Finds stories, addressing mobility through people and object biographies. Archaeological Museum in Zagreb, 17–30.

FARRANT, A.R. & SMART, P.L. (2011): Role of sediment in speleogenesis; sedimentation and paragenesis.– Geomorphology, 134, 79–93. doi: 10.1016/j.geomorph.2011.06.006

GABROVŠEK, F., DREYBRODT W. & PERNE, M. (2010): Physics of condensation corrosion in caves.– In: CARRASCO, F., VALSERO, J.J.D. & LAMOREAUX, J.W. (eds.): Advances in research in karst media. Springer, Berlin, Heidelberg, 491–496. doi: 10.1007/978-3-642-12486-0_75

GARAŠIĆ, M. (1991): Morphological and hydrogeological classification of speleological structures (caves and pits) in the Croatian karst area.– Geološki vjesnik, 44, 289–300.

GARAŠIĆ, M. (2021): The Dinaric Karst System of Croatia: Speleology and Cave Exploration.– Springer International Publishing, 462 p. doi: 10.1007/978-3-030-80587-6

GINÉS, J. (1995): L'endocarst de Mallorca: els mecanismes espeleogenètics/ Mallorca's endokarst the speleogenetic mechanisms.– Endins: publicació d'espeleologia, 71–86.

HAMMER, Ø., HARPER, D.A. & RYAN, P. (2001): PAST: Paleontological Statistics Software Package for Education and Data Analysis.– Palaeontologia Electrónica, 4, 1–9.

HÄUSELMANN, P. (2011): UIS mapping grades.– International Journal of Speleology, 40/2, 15.

JOUVES, J., VISEUR, S., ARFIB, B., BAUDEMENT, C., CAMUS, H., COLLON, P. & GUGLIELMI, Y. (2017): Speleogenesis, geometry, and topology of caves: A quantitative study of 3D karst conduits.– Geomorphology, 298, 86–106. doi: 10.1016/j.geomorph.2017.09.019

LAURITZEN, S. & LAURITSEN, A. (1995): Differential diagnosis of paragenetic and vadose canyons.– Cave and Karst Science 21/2, 55–59.

LAURITZEN, S. & LUNDBERG, J. (2000): Solutional and erosional morphology of caves.– In: KLIMCHOUK, A., FORD, D.C., PALMER, A.N. & DREYBRODT, W. (eds.): Speleogenesis. Evolution of Karst Aquifers. Huntsville, National Speleological Society.

LAZARIDIS, G.T. (2022): Definition and process-based classification of caves.– Acta Carsol., 51/1, 65–77. doi: 10.3986/ac.v51i1.10611

LITTVA, J., HOK, J. & BELLA, P. (2015): Cavitonics: Using caves in active tectonic studies (Western Carpathians, case study).– Journal of Structural Geology, 80, 47–56. doi: 10.1016/j.jsg.2015.08.011

MARINČIĆ, S. (1997): Tectonic structure of the island of Hvar (southern Croatia).– Geologia Croatica, 50/1, 57–77.

MARJANAC, S. (1956): Pećine i jame otoka Lastova.– Speleolog, 4/1–2, 10–19.

OSBORNE, R.A.L. (2002): Cave breakdown by vadose weathering.– Int. J. Speleol., 31/1, 37–53. doi: 10.5038/1827-806X.31.1.3

PASINI, G. (2009): A terminological matter: paragenesis, antigravitative erosion or antigravitational erosion?– International Journal of Speleology, 38/2, 129–138. doi: 10.5038/1827-806X.38.2.4

PICCINI, L. (2011): Recent developments on morphometric analysis of karst caves.– Acta Carsologica, 40/1. doi: 10.3986/ac.v40i1.27

PLAN, L., FILIPPONI, M., BEHM, M., SEEBACHER, R. & JEUTTER, P. (2009): Constraints on alpine speleogenesis from cave morphology – a case study from the eastern Totes Gebirge (Northern Calcareous Alps, Austria).– Geomorphology, 106/1–2, 118–129. doi: 10.1016/j.geomorph.2008.09.011

SHANOV, S. & KOSTOV, K. (2014): Dynamic tectonics and karst.– Springer, 123 p. doi: 10.1007/978-3-662-43992-0

SOKAČ, B., GRGASOVIĆ, T. & HUSINEC, A. (2014): *Clypeina lagustensis* n. sp., a new calcareous alga from the Lower Tithonian of the Lastovo Island (Croatia).– Geologia Croatica, 67/2, 75–86. doi: 10.4154/GC.2014.06

SURIĆ, M., LONČARIĆ, R. & LONČAR, N. (2010): Submerged caves of Croatia: distribution, classification and origin.– Environmental Earth Sciences, 61, 1473–1480. doi: 10.1007/s12665-010-0463-0

SZCZYGIEŁ, J., SOBCZYK, A., MACIEJEWSKI, M. & FERNANDEZ, O. (2022): Variscan vs. Alpine structural controls: Karstic proto-conduit development within Palaeozoic marble post-conditioned by Alpine faulting (the Niedźwiedzia Cave, NE Bohemian Massif).– Geomorphology, 415, 108423. doi: 10.1016/j.geomorph.2022.108423

VLAHOVIĆ, I., TIŠLJAR, J., VELIĆ, I. & MATIČEC, D. (2002): The Karst Dinarides are composed of relics of a single Mesozoic platform: facts and consequences.– Geologia Croatica, 55/2, 171–183.

VLAHOVIĆ, I., TIŠLJAR, J., VELIĆ, I. & MATIČEC, D. (2005): Evolution of the Adriatic carbonate platform: palaeogeography, main events and depositional dynamics.– Paleogeography Paleoclimatology Paleoecology, 220, 333–360. doi: 10.1016/j.palaeo.2005.01.011

WHITE, E. & WHITE, W. (2000): Breakdown morphology.– In: KIMCHOUK, A.B., FORD, D.C., PALMER, A.N. & DREYBRODT, W. (eds.): Speleogenesis: Evolution of karst aquifers. Huntsville, National Speleological Society, 2000, 427–429.

ZACZEK-PEPLINSKA, J. & KOWALSKA, M. (2022): Evaluation of the LiDAR in the Apple iPhone 13 Pro for use in Inventory Works.– In: XXVII FIG Congress, 11–15.

Supplement 1.

Table S1. Analytic presentation of measured discontinuities in the dataset "limestone".

Structural element	Measured surfaced
Bedding	22
Joint set J_1	19
Joint set J_2	11

Table S2. Dataset of limestone discontinuities measured on the surface above the cave.

planeType	dip	dipAzimuth	strike
Joint	70.1904	183.722	93.72202
Joint	71.92961	186.2168	96.21678
Joint	60.76754	192.3736	102.3736
Joint	62.6535	192.4151	102.4151
Joint	64.44534	193.5039	103.5039
Joint	77.69932	197.5304	107.5304
Joint	68.17551	198.4231	108.4231
Joint	74.88907	199.1452	109.1452
Joint	58.83289	199.8249	109.8249
Joint	63.27093	199.9023	109.9023
Joint	69.60873	200.4109	110.4109
Joint	85.67558	200.4482	110.4482
Joint	71.74333	201.4845	111.4845
Joint	57.07592	203.2287	113.2287
Joint	54.55397	204.0684	114.0684
Joint	66.88847	205.9646	115.9646
Joint	65.23213	216.743	126.743
Joint	87.45946	222.5092	132.5092
Joint	50.05435	230.8193	140.8193
Joint	72.88331	111.2763	201.2763
Joint	72.42332	292.5967	202.5967
Joint	72.5682	295.1761	205.1761
Joint	73.54114	295.1895	205.1895
Joint	84.91031	295.4134	205.4134
Joint	86.36198	296.3551	206.3551
Joint	86.05621	117.4916	207.4916
Joint	80.64629	302.1627	212.1627
Joint	77.13354	302.394	212.394
Joint	75.96823	123.3732	213.3732
Joint	87.56434	304.0756	214.0756
Bedding	33.92595	11.76361	281.7636
Bedding	18.18498	13.17101	283.171
Bedding	49.6176	22.13975	292.1398
Bedding	43.83539	33.53652	303.5365
Bedding	17.92305	35.95442	305.9544
Bedding	34.05956	37.33838	307.3384
Bedding	24.52202	39.90214	309.9021
Bedding	24.21395	40.07541	310.0754
Bedding	21.47653	42.40966	312.4097
Bedding	23.21844	46.46361	316.4636
Bedding	25.54895	46.49007	316.4901
Bedding	21.27693	46.68997	316.69
Bedding	26.13662	47.05231	317.0523
Bedding	21.49175	50.81533	320.8153
Bedding	24.11968	50.95646	320.9565
Bedding	23.2489	53.51107	323.5111
Bedding	15.40437	56.47585	326.4758
Bedding	21.90978	56.59077	326.5908
Bedding	20.95658	56.98454	326.9845
Bedding	20.81037	57.46151	327.4615
Bedding	15.07527	62.99094	332.9909
Bedding	14.88991	76.0735	346.0735

Table S3. Dataset of randomly measured wall and ceiling surfaces inside the cave.

dip	dipAzimuth	strike
51.81017685	25.68552208	295.6855
38.88447952	340.7792358	250.7792
34.71315765	17.41595268	287.416
52.15966415	16.62786484	286.6279
47.99376678	353.7681274	263.7681
48.86156464	347.1168823	257.1169
60.07530594	13.40961266	283.4096
46.13370514	348.4091187	258.4091
43.0787735	2.44380283	272.4438
54.68507385	289.0726013	199.0726
50.70658493	38.46739197	308.4674
46.82404327	23.12981987	293.1298
45.12934875	32.50724792	302.5073
34.96255875	21.45202637	291.452
30.47458839	24.12602997	294.126
43.03783417	353.1479492	263.1479
43.27635574	354.4704285	264.4704
46.67576599	5.80060196	275.8006
79.74478912	359.5907593	269.5908
38.39340973	32.11775589	302.1178
43.78738022	1.73403418	271.734
47.98820877	22.04389	292.0439
53.92189026	58.53795242	328.538
15.10485268	74.88994598	344.89
55.31650925	274.9995422	184.9995
56.0885582	231.2857666	141.2858
34.16085052	182.554245	92.55425
11.69459152	57.89809036	327.8981
40.20506668	176.2858124	86.28581
86.48286438	341.5631409	251.5631
80.80680847	176.1418762	86.14188
80.18000793	175.7680359	85.76804
44.0525589	188.3782349	98.37823
16.46254921	192.9366455	102.9366
41.74983597	192.8010559	102.8011
37.04017639	202.0323181	112.0323
50.96066284	196.0754395	106.0754
51.62998581	197.9461517	107.9462
6.95496511	114.7550278	24.75503
35.15284348	197.7796936	107.7797
53.35619354	172.0287781	82.02878
63.40547562	203.5804443	113.5804
38.98209763	189.9543915	99.95439
36.01334763	189.4803619	99.48036
26.29405022	178.7600708	88.76007
47.84452438	184.2487488	94.24875
42.01301956	179.4407654	89.44077
51.16294861	179.5746765	89.57468
61.87059021	176.6659546	86.66595
55.70941544	169.532074	79.53207
18.06053925	103.279274	13.27927
30.76000023	168.9787598	78.97876
22.31475639	152.1667175	62.16672
12.49810219	85.66561127	355.6656
51.95710754	147.5499573	57.54996
17.23378563	41.6733284	311.6733
43.19434357	196.2207336	106.2207

Table S3. Continued.

64.37724304	182.5814514	92.58145	37.30485153	22.42285919	292.4229
43.95110321	185.7926483	95.79265	87.18093872	349.376648	259.3766
16.25034142	10.27902889	280.279	22.72686386	23.99195671	293.9919
48.64162827	180.4055176	90.40552	45.86300278	14.26215935	284.2621
57.17521667	180.3766937	90.37669	87.20011902	329.190033	239.19
50.62455368	128.3023834	38.30238	83.81307983	335.3583984	245.3584
37.45290375	176.8956909	86.89569	44.34930038	11.4164257	281.4164
52.34550476	169.4284363	79.42844	20.08646393	30.0602951	300.0603
21.38539886	36.22367477	306.2237	54.93972778	5.80375576	275.8038
62.66679764	163.6212921	73.62129	51.82859802	36.19450378	306.1945
89	163.9104157	73.91042	27.45674896	33.88423157	303.8842
65.28587341	176.6878815	86.68788	11.77245617	43.2335968	313.2336
69.71627045	170.976471	80.97647	5.56982136	340.2375794	250.2376
51.29399872	165.8537598	75.85376	53.21250534	23.3540554	293.3541
14.28626442	29.36658859	299.3666	35.98528671	24.30040359	294.3004
66.05008698	165.7699432	75.76994	42.97766876	38.8841629	308.8842
56.39934158	118.6528854	28.65289	28.94192314	314.7141113	224.7141
25.03895378	6.43108511	276.4311	19.21271324	243.3904572	153.3905
70.78977966	95.69387054	5.693871	38.65695953	35.6414032	305.6414
54.30705261	135.006073	45.00607	73.00608826	125.1915512	35.19155
73.24403381	315.0262451	225.0262	50.79981613	196.4559631	106.456
85.31558228	301.187439	211.1874	74.38387299	121.3219833	31.32198
41.76155853	124.7254257	34.72543	28.61218643	23.44040871	293.4404
38.45618439	157.5586548	67.55865	37.10426712	153.8766785	63.87668
51.37637329	99.48777771	9.487778	44.60998154	151.1885681	61.18857
50.13928604	135.6249085	45.62491	46.7310257	22.80583572	292.8058
61.85085297	144.1279602	54.12796	27.00732613	121.293747	31.29375
68.43937683	87.5002594	357.5002	38.61858749	124.3654327	34.36543
43.7901001	62.85770798	332.8577	42.93967056	117.3129196	27.31292
72.55857849	118.746788	28.74679	56.49079895	123.5715027	33.5715
61.11566925	149.2992249	59.29922	36.60788345	158.1975555	68.19756
51.21696472	136.0491486	46.04915	35.08895874	158.9268341	68.92683
51.47016525	133.4876251	43.48763	20.82408524	152.7225952	62.7226
79.19998932	266.4174194	176.4174	31.75463486	18.40585899	288.4059
87.05994415	339.9796753	249.9797	46.60958099	206.6821899	116.6822
83.25766754	318.3826294	228.3826	38.52404785	16.68103218	286.681
32.68767929	14.32559872	284.3256	80.98046112	124.2035065	34.20351
22.32835007	7.10480309	277.1048	43.18328857	204.8309326	114.8309
36.77183151	2.26389885	272.2639	14.6488924	36.44748306	306.4475
46.52796555	29.3073349	299.3073	18.79786301	51.42290497	321.4229
35.97826767	29.97133255	299.9713	37.2375946	26.81740189	296.8174